Electromagnetic Metamaterials for Terahertz Applications

Hou-Tong Chen[1], Willie J. Padilla[2], Richard D. Averitt[3],
Arthur C. Gossard[4], Clark Highstrete[5], Mark Lee[5],
John F. O'Hara[1], and Antoinette J. Taylor[1]

[1]MPA-CINT, MS K771, Los Alamos National Laboratory, Los Alamos, NM 87545, USA
[2]Department of Physics, Boston College, 140 Commonwealth Ave., Chestnut Hill, MA 02467, USA
[3]Department of Physics, Boston University, 590 Commonwealth Ave., Boston, MA 02215, USA
[4]Materials Department, University of California, Santa Barbara, CA 93106, USA
[5]Sandia National Laboratories, P.O. Box 5800, Albuquerque, NM 87185-1415, USA
Email: chenht@lanl.gov

Abstract: The recently developed class of artificially structured composite materials, termed metamaterials, has shown increasing importance in accomplishing necessary functional devices for THz applications. We have created a series of novel planar electric metamaterials operating at THz frequencies. Alteration of substrate properties has resulted in actively and dynamically switchable THz metamaterial devices. High efficiency, all-electronic THz switching and modulation operating at room temperature have been accomplished by the use of a hybrid of metamaterial and Schottky diode structure. Dynamic switching of THz radiation was also achieved by photoexcitation of the semiconductor substrate, where ultrafast switching has been demonstrated by the use of an ErAs/GaAs nanoisland superlattice substrate.
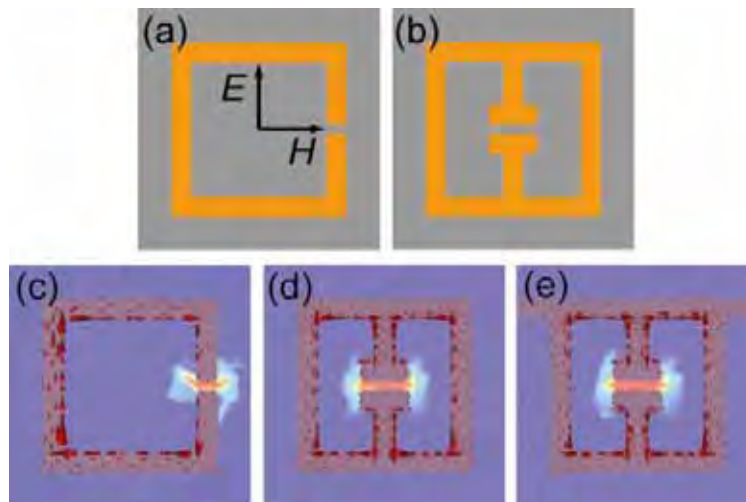
I. Introduction

During the past two decades moderate progress has been achieved in the development of terahertz (THz) science and technology. This may be best represented by the THz time-domain spectroscopy (THz-TDS) [1,2] and the compact solid state THz quantum cascade lasers (THz-QCL) [3,4]. Further accomplishments to fulfill fruitful THz applications, however, are severely restricted mainly due to the deficiency of materials having a suitable response in this frequency range [5]. As compared to the microwave electronic and optical photonic technologies, the development of THz technology is lagging far behind. Functional THz devices such as filters, switches, modulators, and phase-shifting and beam-steering devices, largely are not available.

In addition to actively searching for novel materials, artificial structured materials have played an increasingly important role particularly in the construction of functional THz devices [3,6-8]. This new class of artificial composite materials, termed electromagnetic metamaterials, is constructed to yield a designed resonant response to electromagnetic waves. Metamaterials typically consist of periodically patterned sub-wavelength metallic elements embedded within or on top of a dielectric substrate, and offer an electromagnetic response that is difficult or impossible to obtain from natural occurring materials. Metamaterials have recently attracted enormous attention and growth due to the demonstration of exotic effects such as negative refractive index [9-11], perfect focusing [12,13], and invisibility cloaking [14,15].

   A great deal of metamaterials research has been focused in the microwave frequency range [10] due in part to the ease of fabrication of sub-wavelength structures at these frequencies. Metamaterials are scalable, which has demonstrated operability over many decades of electromagnetic spectrum from RF to optical frequencies [16-19]. Although currently most effort in metamaterials research is focused on higher optical frequencies [20], less work has concentrated on THz frequencies. However, the potential uses of metamaterials in this frequency range offer a great promise that alleviates the limitations of natural materials. In this paper we present a brief review of our recent progress in the novel THz metamaterials [21,22]. Functionalizing the metamaterials is achieved by either active or dynamic modification of the surrounding environment using external electrical or optical stimuli. With such approaches we have demonstrated all-electronically and ultrafast dynamically switchable THz metamaterial devices [6,7,23].

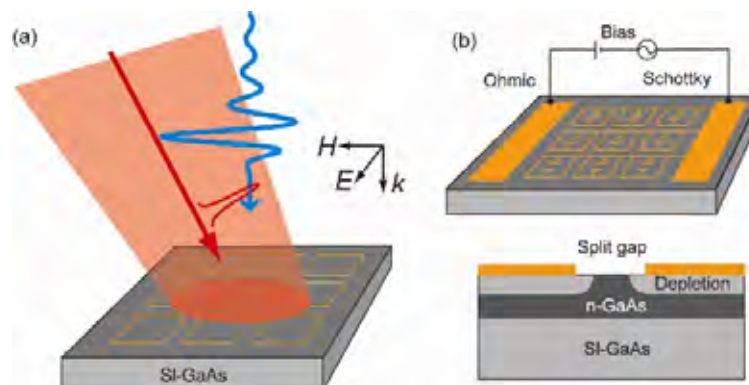## II. Sample design and fabrication

Fig. 1 (a) Schematics of planar metamaterials consist of unit cells (a) a split-ring resonator (SRR), and (b) an electric split-ring resonator (eSRR). Numerical simulation results for (c) SRR, (d) eSRR, and (e) eSRR with connecting wires. The arrows indicate the surface current density, and the colors map the electric field norm.

   In Fig. 1 we show the unit cells of (a) a split-ring resonator (SRR) and (b) a so-called electric split-ring resonator (eSRR) [21,22,24], which were drawn in scale, with split gaps of 2 μm, a metal linewidth of 4 μm, and an outer dimension of 36 μm. Planar metamaterials form when they are periodically patterned on a suitable substrate, where the individual unit cell is repeated in a simple square array geometry with a sub-wavelength lattice parameter of $a = 50$ μm. Typically $a \sim \lambda_0 / 10$ where λ_0 is the wavelength at the resonance frequency ω_0. The operation principle for both designs is similar. The metallic loops of the SRR or eSRR are effectively inductors, L, and the split gaps provide capacitors, C. Then the devices can be equivalent to lumped LC resonator

arrays, and the resonance frequency is determined by $\omega_0 \sim (LC)^{-1/2}$. The polarization of the normally incident THz radiation is also shown in Fig. 1. With such configurations we characterize the electric response, which is properly represented by an effective complex dielectric function $\tilde{\varepsilon}(\omega)$. It is the THz electric field instead of the magnetic field (which is in the plane of metamaterial elements) that drives the metamaterial resonance response.

In order to obtain certain functionalities, we fabricated planar metamaterials on semiconductor substrates, where the conductivity can be externally modified either by an optical excitation or applying a voltage bias. We used the unit cell in Fig. 1(a) for the dynamically switchable metamaterials, which were fabricated on a semi-insulating gallium arsenide (SI-GaAs) substrate of 670 μm thickness, shown in Fig. 2(a). The planar array of SRRs was fabricated from 3 μm thick copper. The fabrication of the ultrafast optically switchable THz metamaterial devices was a little different. Here we used the unit cell shown in Fig. 1(b) and an ErAs/GaAs nanoisland superlattice substrate. The planar metamaterials were fabricated using the standard photolithographic methods and the metallization is achieved by the electron beam deposition of 10 nm thick titanium as the adhesion layer, following 200 nm thick gold layer, and then performed a lift-off process.

Fig. 2 Schematics of externally controllable THz metamaterial devices. (a) The dynamically switchable THz metamaterial device upon femtosecond photoexcitation fabricated on an SI-GaAs substrate. (b) The all-electronically switchable THz metamaterial device fabricated on GaAs substrate with an *n*-type doped layer. The depletion regions (bottom) can be modified by applying a reverse voltage bias (top) to switch the metamaterial resonance.

The substrate used for the all-electronically switchable metamaterial devices has a 1-μm-thick *n*-doped GaAs layer grown by molecular beam epitaxy (MBE) on an SI-GaAs substrate. The fabrication started with an ohmic electrical pad, which was metalized by electron beam deposition of 20 nm of germanium, 20 nm of nickel, and 200 nm of gold in sequence, and then performed a rapid thermal annealing (RTA) process at 350°C for 1 minute. Then the metallic eSRRs array was fabricated using standard photolithographic methods and electron beam deposition of 10 nm of titanium and 200 nm of gold. Here we used the unit cell shown in Fig. 1(b) and all eSRRs were connected together with metallic wires as shown in Fig. 2(b).

III. Experimental techniques

We characterized the frequency-dependent electric response of the above metamaterial devices using THz time-domain spectroscopy (THz-TDS). The linearly polarized, normally incident, impulsive THz electric field was measured after propagating through the samples and a suitable reference. Fourier transformation allows us to obtain the THz spectra that contain both amplitude and phase information. Dividing the sample spectrum by the reference yields a complex transmissivity $\tilde{t}(\omega) = t(\omega)e^{i\phi(\omega)}$ of the metamaterial, which further permits calculation of optical constants, e.g., the effective complex dielectric function $\tilde{\varepsilon}(\omega) = \varepsilon_1(\omega) + i\varepsilon_2(\omega)$, through the inversion of Fresnel equations without model assumptions.
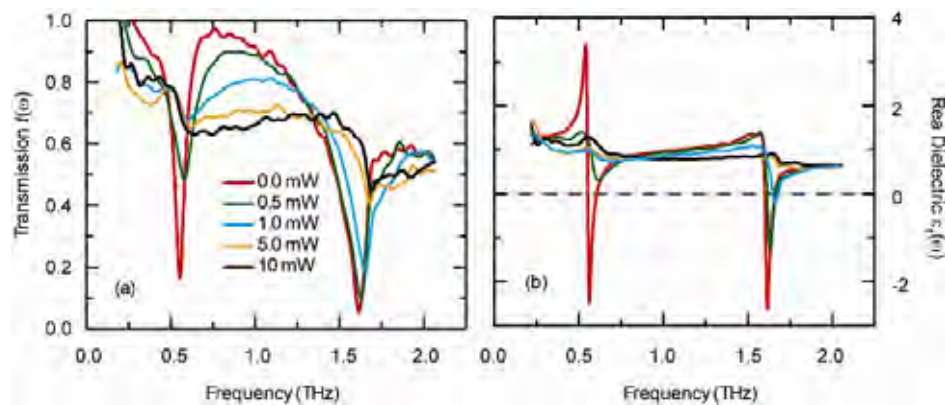
The dynamically switchable THz metamaterial devices were characterized using optical-pump terahertz-probe (OPTP) spectroscopy [25], schematically shown in Fig. 2(a). The synchronized femtosecond optical pulses with pulse duration of ~50 fs, a pulse repetition rate of 1 kHz, and a center wavelength of 800 nm, are expanded larger than the THz focal spot at the samples to uniformly excite free charge carriers in the semiconductor substrate. We performed THz transmission measurements through metamaterials upon various photoexcitation fluences, which occurs several picoseconds before the arrival of the THz pulse. The carrier lifetime in SI-GaAs is orders of magnitude longer than the picosecond duration of THz pulses, which allows for characterization of a quasi-steady state response of metamaterials. For metamaterials fabricated on ErAs/GaAs nanoisland superlattice substrates where the carrier lifetime is ~10 ps, we varied the time delay between the photoexcitation and THz arrival so that the metamaterial dynamic response upon photoexcitation can be measured. In these measurements, we used a bare SI-GaAs or ErAs/GaAs superlattice substrate as the reference. For the electronically switchable metamaterial devices, using a standard photoconductive THz-TDS experimental system [26] we performed THz transmission measurements as a function of voltage bias applied to the devices, shown in Fig. 2(b). All the above measurements were performed at room temperature in a dry air atmosphere.

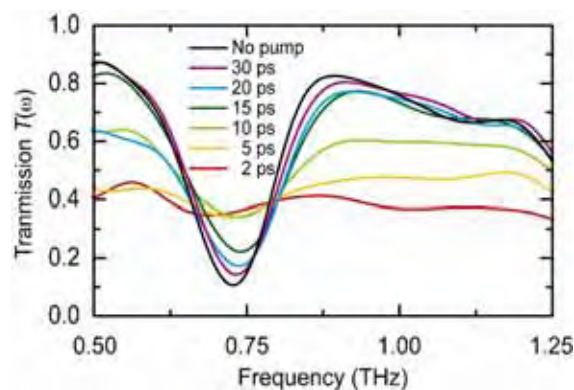### IV. Dynamic THz metamaterial devices: Ultrafast switching of THz radiation

In Fig. 3 we show the electromagnetic response of SRRs array fabricated on semiconductor substrate. In Fig. 3(a) the transmission of THz electric field was plotted for varying photoexcitation fluences, and in Fig. 3(b) we show the corresponding extracted the real portion of the effective complex dielectric function $\varepsilon_1(\omega)$. With no photoexcitation, the THz transmission through the metamaterial is shown as the red curve in Fig. 3(a). While off-resonance, the transmission amplitude $t(\omega)$ has relatively high values near 95%, and near 0.5 THz the transmission drops to ~20%. This transmission minimum is associated with the THz electric field driven circulating currents resonating in SRRs, as verified by the numerical finite-element simulation shown in Fig. 1(c). This electric resonance response has the same resonance frequency as in the magnetic

resonance response [27] using the same metamaterial structure. There is a second resonant THz transmission minimum near 1.6 THz. This resonance is from the half wave resonance of the side length 36 μm of SRRs, as verified by the numerical simulation (not shown). Below we solely discuss the first resonance near 0.5 THz.

Photoexcitation with near-infrared laser pulses creates free charge carriers in the SI-GaAs substrate. The photocarriers in the GaAs substrate short the split gaps of SRRs, thereby damping the resonance response of the metamaterial. As shown in Fig. 3(a), the resonance behavior changes dramatically with the increasing photoexcitation fluence. Under as low as 1 mW photoexcitation fluence, which corresponds to 2 μJ/cm^2 or equivalently to a photoexcited carrier density of ~4$\times$10^{16} cm^{-3}, the resonance has been completely damped. In Fig. 3(b) we show the corresponding extracted real part of the effective complex dielectric function $\varepsilon_1(\omega)$. Using photoexcitation we are able to switch the permittivity $\varepsilon_1(\omega)$ from negative to positive values near the resonance.

Fig. 3 (a) Frequency-dependent transmission of the THz electric field and (b) the corresponding real part of the effective complex dielectric function upon various photoexcitation fluences for the metamaterial fabricated on an SI-GaAs substrate. The polarization of the normally incident THz radiation has been shown in Fig. 2.
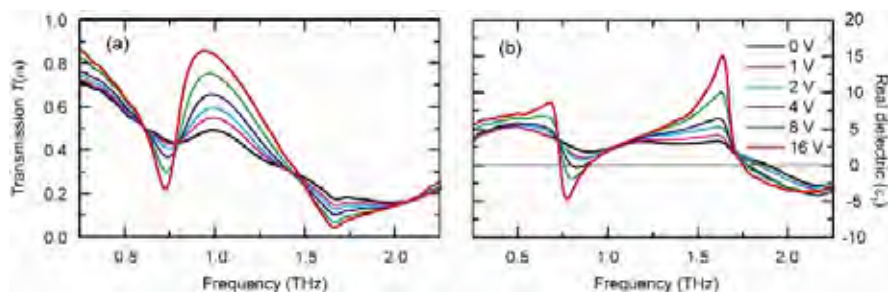

Fig. 4 Frequency-dependent transmission of the THz intensity with various time delays following the photoexcitation for the metamaterial fabricated on an ErAs/GaAs nanoisland superlattice substrate.

The dynamic switching off of the metamaterial resonance response could be very fast, i.e., only depending on the femtosecond photoexcitation of charge carriers. The switching recovery time, however, is determined by the carrier lifetime, which could be as long as a nanosecond in the GaAs substrate. In order to realize ultrafast switching recovery, it is obvious that the carrier lifetime needs to be significantly shortened. There are some candidate materials such as radiation-damaged silicon, low temperature grown gallium arsenide, and ErAs/GaAs nanoisland superlattices. We used ErAs/GaAs nanoisland superlattice [28] as the metamaterial substrate, where the carrier lifetime is strongly correlated with the period of the superlattice. In this work, 20 periods with 100 nm each results in a carrier lifetime of approximately 10 ps. Such carrier lifetime is ideal to demonstrate the ultrafast switching of THz metamaterials due to the picosecond duration of THz pulses. The experimental results are shown in Fig. 4. With no photoexcitation, the metamaterials show strong resonance transmission dip. When the THz pulses arrive immediately after the photoexcitation (less than 5 ps), the excited photocarriers short the split gaps thereby almost completely eliminating the metamaterial resonance response. Increasing the time delay between the photoexcitation and the arrival of THz pulses, however, allows for the carrier recombination and the recovery of the resonance. At a time delay of ~20 ps the resonance has been almost completely recovered.

V. Active THz metamaterial devices: All-electronic switching of THz radiation

When the metallic eSRRs are fabricated on an *n*-type GaAs substrate, the metal-semiconductor interface forms a Schottky diode structure. The depletion regions underneath and around the metal, particularly near the split gaps, can be actively controlled by applying a voltage bias between the metal and substrate. In this way we can effectively control the conductivity of the substrate near the split gaps, which in turn switches the resonance of eSRRs. In Fig. 5 we show the experimental results of transmission of THz intensity as a function of the applied reverse voltage bias to the active metamaterial device shown in Fig. 2(b). With no voltage bias the metamaterial resonance response is strongly damped due to the conducting and lossy substrate, i.e., the split gaps of eSRRs are shortened by the relatively conducting substrate. As shown by the black curves in Fig. 5, we only observed very weak and broad resonance THz

Fig. 5 Switching performance of the active THz metamaterial device as a function of reverse voltage bias. (a) Frequency-dependent transmission of the THz intensity, and (b) the corresponding extracted real part of the effective complex dielectric function. The polarization of the normally incident THz radiation has been shown in Fig. 2.

transmission dip, and the Lorentz-like dispersion was barely seen in the extracted effective dielectric function $\varepsilon_1(\omega)$.

A reverse voltage bias, on the other hand, drives electrons away from the interface and increases the width of depletion regions. This isolates the metal from the doped semiconductor substrate, and particularly, recovers the split gaps. As shown in Fig. 5 we observed that, with an increasing reverse voltage bias, the metamaterial resonance response is reestablished, i.e. increasing resonance strength and a narrowing resonance linewidth, and the strong Lorentz-like dispersion $\varepsilon_1(\omega)$ associated with the resonance. Under a reverse voltage bias of 16 volts, a switching efficiency of 50% in THz intensity can be achieved at room temperature. This represents one order of magnitude improvement over the previous electrically driven THz switch based on a HEMT structure [29]. Additionally, the effective real part of the complex dielectric function $\varepsilon_1(\omega)$ is switched between positive and negative values.

In the all-electronic switchable THz metamaterial devices, it is necessary to connect all eSRRs together serving as a Schottky contact. So, the symmetric design of eSRRs is of particular importance to avoid any effect on changing the resonance behavior by the connecting wires. In Fig. 1(d) and (e) we show the numerical simulation results of the surface current density as well as the electric field norm at resonance of the eSRR, with or without the connecting wires. There is neither a shift of the resonance frequency nor a change of resonance strength of the eSRR by the connecting wires. It is also worth mention that the connecting wires should be perpendicular to the proposed polarization of the THz electric field to avoid otherwise acting as a filter.

VI. Summary

In this paper we have demonstrated active and dynamic control over the metamaterial devices at THz frequencies. The dynamically switchable THz metamaterials were fabricated on intrinsic GaAs substrate. The photoexcitation of free charge carriers shorts the split gaps and damps the metamaterial resonant response. Using an ErAs/GaAs nanoisland superlattice substrate with very short carrier lifetime, we achieved an ultrafast switching recovery of the metamaterial resonance. The all-electronically switchable THz metamaterial devices are the hybrid of a Schottky diode structure and an eSRR array. Upon applying a reverse voltage bias the depletion regions, particularly near the split gaps, can be actively controlled. We accomplished a switching efficiency up to 50% in the transmission of THz intensity, an order of magnitude improvement over the state of the art. Metamaterials are geometrically scalable to translate the operability over many decades of frequency. The choice of substrate and the capability of modifying substrate properties add great flexibility and make metamaterials promise for practical applications.

References

[1] D. Grischkowsky, S. Keiding, M. van Exter, and Ch. Fattinger, "Far-infrared time-domain spectroscopy with terahertz beams of dielectrics and semiconductors," *J. Opt. Soc. Am. B* 7, 2006-2015, (1990).

[2] Q. Wu, M. Litz, and X.-C. Zhang, "Broadband detection capability of ZnTe Electro-optic field detectors," *Appl. Phys. Lett.* 68, 2924-2926, (1996).

[3] R. Köhler, A. Tredicucci, F. Beltram, H. E. Beere, E. H. Linfield, A. G. Davies, D. A. Ritchie, R. C. Iotti, and F. Rossi, "Terahertz semiconductor-heterostructure laser," *Nature* 417, 156-159, (2002).

[4] B. S. Williams, H. Callebaut, S. Kumar, Q. Hu, and J. L. Reno, "3.4-THz quantum cascade laser based on longitudinal-optical-phonon scattering for depopulation," *Appl. Phys. Lett.* 82 1015-1017, (2003).

[5] B. Ferguson and X.-C. Zhang, "Materials for terahertz science and technology," *Nature Mater.* 1, 26-33, (2002).

[6] W. J. Padilla, A. J. Taylor, C. Highstrete, M. Lee, and R. D. Averitt, "Dynamical electric and magnetic metamaterial response at terahertz frequencies," *Phys. Rev. Lett.* 96, 107401, (2006).

[7] H.-T. Chen, W. J. Padilla, J. M. O. Zide, A. C. Gossard, A. J. Taylor, and R. D. Averitt, "Active metamaterial terahertz devices," *Nature* 444, 597-600, (2006).

[8] T. Matsui, A. Agrawal, A. Nahata, and Z. V. Vardeny, "Transmission resonances through aperiodic arrays of subwavelength apertures," *Nature* 446, 517-521, (2007).

[9] V. G. Veselago, "The electrodynamics of substances with simultaneously negative values of ε and μ," *Sov. Phys. Usp.* 10, 509-514, (1968).

[10] D. R. Smith, W. J. Padilla, D. C. Vier, S. C. Nemat-Nasser, and S. Schultz, "Composite medium with simultaneously negative permeability and permittivity," *Phys. Rev. Lett.* 84, 4184-4187, (2000).

[11] R. A. Shelby, D. R. Smith, and S. Schultz, "Experimental verification of a negative index of refraction," *Science* 292, 77-79, (2001).

[12] J. B. Pendry, "Negative refraction makes a perfect lens," Phys. Rev. Lett. 85, 3966-3969, (2000).

[13] N. Fang, H. Lee, C. Sun, and X. Zhang, "Sub-diffraction-limited optical imaging with a silver superlens," *Science* 308, 534-537, (2005).

[14] J. B. Pendry, D. Schurig, and D. R. Smith, "Controlling electromagnetic fields," *Science* 312 1780-1782, (2006).

[15] D. Schurig, J. J. Mock, B. J. Justice, S. A. Cummer, J. B. Pendry, A. F. Starr, and D. R. Smith, "Metamaterial electromagnetic cloak at microwave frequencies," *Science* 314, 977-980, (2006).

[16] T. J. Yen, W. J. Padilla, N. Fang, D. C. Vier, D. R. Smith, J. B. Pendry, D. N. Basov, and X. Zhang, "Terahertz magnetic response from artificial materials," *Science* 303 1494-1496, (2004).

[17] S. Zhang, W. Fan, N. C. Panoiu, K. J. Malloy, R. M. Osgood, and S. R. J. Brueck, "Experimental demonstration of near-infrared negative-index metamaterials," *Phys. Rev. Lett.* 95, 137404, (2005).

[18] J. Zhou, Th. Koschny, M. Kafesaki, E. N. Economou, J. B. Pendry, and C. M. Soukoulis, "Saturation of the magnetic response of split-ring resonators at optical frequencies," *Phys. Rev. Lett.* 95, 223902 ,(2005).

[19] A. N. Grigorenko, A. K. Geim, H. F. Gleeson, Y. Zhang, A. A. Firsov, I. Y. Khrushchev, and J. Petrovic, "Nanofabricated media with negative permeability at visible frequencies," *Nature* 438, 335-338, (2005).

[20] V. M. Shalaev, "Optical negative-index metamaterials," *Nature Photon.* 1, 41-48, (2007).

[21] W. J. Padilla, M. T. Aronsson, C. Highstrete, M. Lee, A. J. Taylor, and R. D. Averitt, "Electrically resonant terahertz metamaterials: Theoretical and experimental investigations," *Phys. Rev. B* 75, 041102(R), (2007).

[22] H.-T. Chen, J. F. O'Hara, A. J. Taylor, R. D. Averitt, C. Highstrete, M. Lee, and W. J. Padilla, "Complementary planar terahertz metamaterials," *Opt. Express* 15, 1084-1095, (2007).

[23] H.-T. Chen, W. J. Padilla, J. M. O. Zide, S. R. Bank, A. C. Gossard, A. J. Taylor, and R. D. Averitt, "Ultrafast optical switching of terahertz metamaterials fabricated on ErAs/GaAs nanoisland superlattices," *Opt. Lett.* 32, 1620-1622, (2007).

[24] D. Schurig, J. J. Mock, and D. R. Smith, "Electric-field-coupled resonators for negative permittivity metamaterials," *Appl. Phys. Lett.* 88, 041109, (2006).

[25] R. D. Averitt and A. J. Taylor, "Ultrafast optical and far-infrared quasiparticle dynamics in correlated electron materials," *J. Phys.: Condens. Matter* 14, R1357-R1390, (2002).

[26] J. F. O'Hara, J. M. O. Zide, A. C. Gossard, A. J. Taylor, and R. D. Averitt, "Enhanced terahertz detection via ErAs:GaAs nanoisland superlattices," *Appl. Phys. Lett.* 88, 251119, (2006).

[27] W. J. Padilla, "Group theoretical description of artificial electromagnetic metamaterials," *Opt. Express* 15, 1639-1646, (2007).

[28] C. Kadow, S. B. Fleischer, J. P. Ibbetson, J. E. Bowers, A. C. Gossard, J. W. Dong, and C. J. Palmstr m, "Self-assembled ErAs islands in GaAs: Growth and subpicosecond carrier dynamics," *Appl. Phys. Lett.* 75, 3548-3550, (1999).

[29] T. Kleine-Ostmann, P. Dawson, K. Pierz, G. Hein, and M. Koch, "Room-temperature operation of an electrically driven terahertz modulator," *Appl. Phys. Lett.* 84, 3555-3557, (2004).